Carbohydrate Polymers 223 (2019) 115113

Contents lists available at ScienceDirect

Carbohydrate Polymers

journal homepage: www.elsevier.com/locate/carbpol

PEGylated β-cyclodextrins: Click synthesis and in vitro biological insights

Yareli Rojas-Aguirre[a,*], Manuel Alexis Torres-Mena[a], Luis José López-Méndez[a], Sofía L. Alcaraz-Estrada[b], Patricia Guadarrama[a], Juan Manuel Urucha-Ortíz[b]

[a] Instituto de Investigaciones en Materiales, Universidad Nacional Autónoma de México, Mexico City, 04510, Mexico
[b] División de Medicina Genómica, Centro Médico Nacional "20 de Noviembre"-ISSSTE, Mexico City, 03100, Mexico

ARTICLE INFO

Keywords:
Beta-cyclodextrins
Click chemistry
PEGylation
Human monocytes
HeLa
Cells

ABSTRACT

We present three easily rationalized star-shaped PEGylated β-cyclodextrin (βCD) derivatives synthesized via conjugation of different molecular weight PEG chains (5000, 2000, and 550 Da) to the βCD primary face by click chemistry (βCD-PEG$_{5000}$, βCD-PEG$_{2000}$, βCD-PEG$_{550}$ respectively). βCDPEG systems are envisioned to further carry bioactive molecules, therefore, their interactions with biological interfaces must be determined at an early stage of development. Hence, the effect of βCDPEGs chain length on cell viability was investigated. To this aim, three models were selected: Vero cells for their fibroblast-like features; HeLa cells that are commonly used for preliminary viability screening; and human peripheral monocytes which are macrophage precursors. Of the three pegylated derivatives, βCD-PEG$_{550}$ was the one that significantly affected HeLa cells and human monocytes viability. Despite the popularity of PEGylation approach, our results underscore the importance of careful and systematic PEGylated materials design for their future success in drug delivery systems.

1. Introduction

β-Cyclodextrin (βCD) is a cyclic oligosaccharide comprising seven glucopyranose molecules linked through α-1,4 glycosidic bonds. Because of the lack of free rotation of these bonds, the βCD 3D structure is cone-shaped with a hydrophobic cavity and a hydrophilic surface. In this truncated cone, the primary and secondary hydroxyl groups of the glucopyranose units remain on the narrow and wide faces, respectively. βCD is known for forming inclusion complexes with hydrophobic compounds, leading to its successful use in pharmaceuticals (Jambhekar & Breen, 2016). Furthermore, the primary and secondary hydroxyl groups allow for selective chemical modification of the macrocycle, conveying for a range of derivatives with diverse physical and chemical properties and recognition abilities (Khan, Forgo, Stine, & D'Souza, 1998; Řezanka, 2018).

The βCD core can also be functionalized with polymeric moieties, which affords structures with sophisticated supramolecular architectures, specific compositions, and unique characteristics, for instance, mechanical properties and stimuli-responsiveness (temperature, shear forces, pH, etc.). Thus, βCD-based polymeric materials have drawn attention in the drug and gene delivery field, where they have been used to engineer networks and assemblies such as nanogels, nanoparticles, micelles, vesicles, polyplexes, and other complex multifunctional platforms (Antoniuk & Amiel, 2016; Hu, Tang, & Chu, 2014; Jiménez Blanco, Benito, Ortiz Mellet, & García Fernández, 2017; Mellet, Fernández, & Benito, 2011; Schmidt, Hetzer, Ritter, & Barner-Kowollik, 2014; Simões, Rey-Rico, Concheiro, & Alvarez-Lorenzo, 2015; Zhang & Ma, 2013).

Fascinating investigations have shown the potential of βCD-based structures for drug optimization or gene loading and release, with a few examples reaching clinical trials (Sun et al., 2014). However, most βCD supramolecular platforms remain in the proof-of-concept stage. Hence, structurally simple supramolecular systems obtained through facile and clean syntheses and their comprehensive physicochemical and biological evaluations are needed toward tangible applications.

Polyethylene glycol (PEG) is the most investigated synthetic polymer for modifying biomacromolecules and improving drug carrier physicochemical properties (Owens & Peppas, 2006). PEG can function as a bridge to attach drugs or targeting ligands to the carrier, a building block for supramolecular assemblies, or simply as a nanomaterial stabilizer (Knop, Hoogenboom, Fischer, & Schubert, 2010).

Copper(I)-catalyzed azide−alkyne cycloaddition (CuAAC), often referred to as the classic click reaction (both terms will be used interchangeably herein), has succeed in the synthesis of a variety of small

Abbreviations: CuAAC, copper(I)-catalyzed azide−alkyne cycloaddition; βCD, β-cyclodextrin; DCC, *N,N'*-dicyclohexylcarbodiimide; DMAP, 4-(dimethylamino) pyridine; DCU, dicyclohexylurea; FBS, fetal bovine serum; MALDI-TOF, matrix-assisted laser desorption/ionization time-of-flight; PEG, polyethyleneglycol

* Corresponding author.
E-mail address: yareli.rojas@materiales.unam.mx (Y. Rojas-Aguirre).

https://doi.org/10.1016/j.carbpol.2019.115113
Received 8 May 2019; Received in revised form 12 July 2019; Accepted 19 July 2019
Available online 22 July 2019
0144-8617/

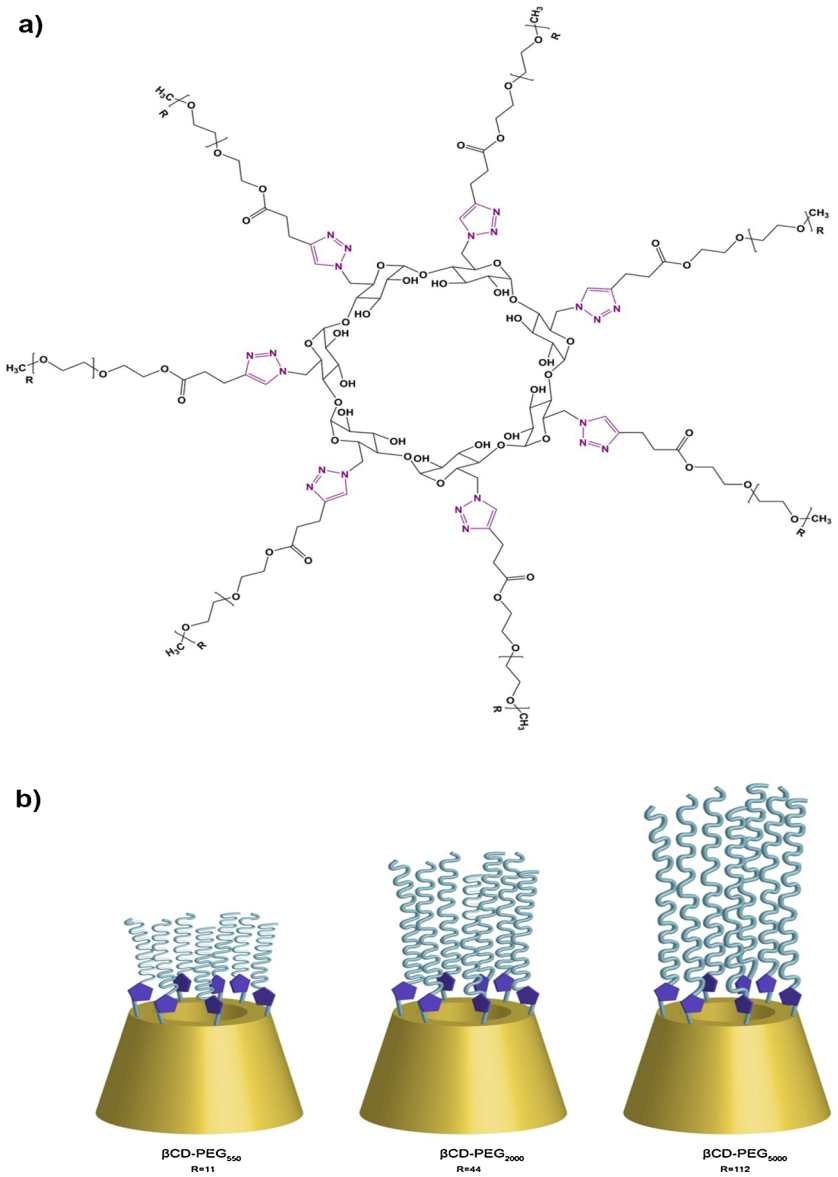

Fig. 1. a) Chemical structure of PEGylated βCDs; b) representation of βCD-PEG$_{550}$, βCD-PEG$_{2000}$, and βCD-PEG$_{5000}$.

molecules and biomacromolecular structures in quantitative yields, without side reactions or tedious purification processes (Meghani, Amin, & Lee, 2017). It has also positively impacted the CD chemistry and led to selective CD functionalization (Buckwalter, Sizovs, Ingle, & Reineke, 2012; Faugeras et al., 2012; Gallego-Yerga et al., 2018; He et al., 2016; López-Méndez et al., 2018).

Thus, we synthesized three easily rationalized star-shaped PEGylated βCD derivatives via the conjugation of PEG chains of different molecular weights to the seven βCD primary face reactive sites by click chemistry (Fig. 1). We selected 2000 and 5000 Da PEG (βCD-PEG$_{2000}$ and βCD-PEG$_{5000}$ respectively) because they are considered as gold standards for physicochemical stabilizers for drug carriers (Davis, 2009; Dos Santos et al., 2007). Additionally, we explored a lower molecular weight PEG (550 Da, βCD-PEG550). In this way, we envisioned asymmetric PEGylated βCDs for their further use as drug carriers, in which the available cavity hosts one drug while PEG allows for attachment of either a second drug or a targeting ligand, namely a multifunctional but simple βCD polymeric structure.

Under this context, we present the synthesis and characterization of βCD-PEG$_{5000}$, βCD-PEG$_{2000}$, and βCD-PEG$_{550}$ and evaluate the scope of click chemistry to obtain each derivative.

When materials are designed for carrying bioactive molecules, like our PEGylated CDs, their interaction with bio-interfaces must be determined. Similarly, it is vital to identify whether the materials induce a toxic cell response at an early development stage before drug loading. Very few PEGylated materials have reached late clinical trials, and detailed research on bridging this gap is highly intriguing (Anselmo & Mitragotri, 2016). Hence, we investigated the effects of the three βCDPEGs, in terms of the influence of different PEG chain lengths, on the in vitro cell viability of Vero and HeLa cells and on human peripheral monocytes. Vero cells, derived from monkey renal epithelial cells, were selected for their fibroblast-like features. They can also provide valuable information about biological responses of mammalian cells in vitro and can be used for preliminary studies of novel materials with biological interfaces (do Nascimento, Ferreira, Malmonge, & Lombello, 2017; Li et al., 2015; Pelegrino et al., 2018).

Yet human HeLa cells are commonly used as cellular models for preliminary screening cytotoxicity, composition and morphology of engineered materials have been shown to influence their biological response. Accordingly, these cells can aid preliminary investigations about biological interactions of new materials (Renero-Lecuna et al., 2019) and they were employed as our second model.

Monocytes are white blood cells belonging to the mononuclear phagocytic system. They migrate toward inflamed tissues, where differentiate into macrophages. Monocytes also internalize and eliminate microorganisms and foreign materials from systemic circulation (Richards & Endres, 2014). They are the first barrier encountered by engineered materials, as they will remove them from the bloodstream before reaching the target site (Owens & Peppas, 2006). PEGylation is the most common approach to overcome this hurdle as it decreases phagocytic cell uptake and increases circulation half-life. However, although PEG has been relatively successful with the liposomal formulation Doxil® (Barenholz, 2012), PEGylated structures can also trigger immune responses and even hinder the efficacy of drug delivery systems (Grenier, Viana, de, Lima, & Bertrand, 2018; Zhang, Sun, Liu, & Jiang, 2016). The investigation of the response of different cells to PEG has gained attention in recent years. However, studies on the effect of PEGylation on primary human cells is scarce with mixed outcomes and they all have been majorly focused on the uptake process. Yang et al. reported that PEG density determines the extent of uptake (Yang et al., 2014), and Farace et al. showed that there is no actual reduction in phagocytic uptake in PEGylated systems (Farace et al., 2016). Any of those studies reported PEG toxicity on phagocytic cells. On the other hand, Kelley et al. found an increased uptake of PEGylated structures by primary human neutrophils and showed that distinct cell types respond differently to PEGylation (Kelley, Fromen, Lopez-Cazares, & Eniola-Adefeso, 2018). This context encouraged us to firstly evaluate the effect of our PEGylated nanostructures on the viability of primary human peripheral monocytes, before studying uptake processes.

Under this context, we hypothesize that: 1) the robustness of click chemistry will allow for straightforward selective attachment of PEG to the seven βCD primary face positions in quantitative yields, regardless of PEG molecular weight; 2) βCDPEG structures, resulting from the combination of two safe components, namely βCD and linear PEG, will not necessarily result in materials with the same biological behavior as their precursors, since the new structure, displaying different physicochemical properties, could induce distinct cellular responses, in this case, viability.

Previously, cationic βCDs were PEGylated in the seven of the 14 secondary rim positions, and the PEG chain length was investigated to determine its influence on macrocycle stability (Godinho et al., 2014; O'Mahony et al., 2012). Here, we PEGylated the primary face of native βCD and explored the effect of PEG length on the viability of different cell lines. To the best of our knowledge, this is the first study of its kind.

2. Experimental

2.1. Materials

Iodine (99% w/w), NaN_3 (99% w/w), triphenylphosphine (≥98% w/w), $CuSO_4{\cdot}H_2O$ (99.99% w/w), L-ascorbic acid (99% w/w), DMAP (99% w/w), DCC (98% w/w), 4-pentynoic acid (95%), PEG methyl ether average M_n 550, 2000, and 5000, methanol (99.8%), dimethyl sulfoxide (DMSO), $CDCl_3$, and DMSO-d_6 were purchased from Sigma-Aldrich and used as received. βCD (98%, Sigma-Aldrich) was dried under vacuum before use. *N*,*N*´-Dimethylformamide (Sigma-Aldrich) and methylene chloride (Sigma-Aldrich) were dried over CaH_2 before use.

Heptakis(6-deoxy-6-iodo)-β-cyclodextrin (βCD-$(I)_7$) and heptakis(6-deoxy-6-azido)-β-cyclodextrin (βCD-$(N_3)_7$) were prepared in our laboratory in accordance to the reported protocols (Gadelle & Defaye, 1991; García Fernández et al., 1995). Spectroscopic data for both, βCD-$(I)_7$ and βCD-$(N_3)_7$, were identical to those previously reported (Supporting information) (Gadelle & Defaye, 1991; García Fernández et al., 1995; López-Méndez et al., 2018).

2.2. Syntheses

2.2.1. Alkyne-functionalized PEG methyl ether M_n 5000

PEG_{5000} (2.0 g, 0.4 mmol) was dissolved in 12 mL of CH_2Cl_2. 4-Pentynoic acid (0.07 g, 0.72 mmol) was added to the PEG_{5000} solution, followed by DMAP (0.49 g, 0.4 mmol). The solution was stirred 5 min at RT, and DCC (0.15 g, 0.72 mmol) dissolved in CH_2Cl_2 (2 mL) was added dropwise. The reaction mixture was stirred overnight at RT. Afterwards, precipitated DCU was removed by filtration through celite, the solvent was rota-evaporated, and the product was re-dissolved in fresh CH_2Cl_2 for extraction with a saturated sodium chloride aqueous solution. The organic phase was dried over Na_2SO_4, and the product was recovered by three-fold precipitation in cold diethyl ether. Alkynyl-PEG_{5000} was filtered and air-dried (1.8 g, 87% yield). $M_{n\text{-theo}}$: 5080.08 g/mol; $M_{n\text{-NMR}}$: 5090.92 g/mol. ^{1}H NMR: 4.24 (t, 2H), 3.79 (t, 2H), 3.62 (m, J = 2.2 Hz, 448H), 3.35 (s, J = 2.1 Hz, 3H), 2.57 (m, 2H), 2.49 (m, 2H), 1.97 (t, 1H).

2.2.2. Alkyne-functionalized PEG methyl ether M_n 2000

The procedure in Section 2.2.1 with PEG_{2000} (2 g, 0.99 mmol), 4-pentynoic acid (0.18 g, 1.79 mmol), DMAP (0.12 g, 0.99 mmol), DCC (0.37 g, 1.79 mmol); CH_2Cl_2 (10 mL). Alkynyl-PEG_{2000} (1.28 g, 72% yield). $M_{n\text{-theo}}$: 2080.08 g/mol; $M_{n\text{-NMR}}$: 2094.84 g/mol. ^{1}H NMR: 4.25 (t, 2H), 3.81 (t, 2H), 3.63 (s, 176H), 3.37 (s, 3H), 2.56 (m, 2H), 2.49 (m, 2H), 1.9 (t, J = 2.6 Hz, 1H).

2.2.3. Alkyne-functionalized PEG methyl ether M_n 550

The procedure in Section 2.2.1 with PEG_{550} (1 mL, 1.94 mmol), 4-pentynoic acid (0.34 g, 3.5 mmol), DMAP (0.24 g, 1.94 mmol), DCC (0.72 g, 3.5 mmol), and CH_2Cl_2 (14 mL). For the reaction workup, the crude product was washed with water, and water-soluble PEG material was recovered into CH_2Cl_2 by salting out. The solvent was vacuum removed, and alkynyl-PEG_{550} was obtained as a pale brown liquid (1.24 g, 97% yield). $M_{n\text{- theo}}$: 630.08; $M_{n\text{-NMR}}$: 640.86. ^{1}H NMR: 4.26 (t, 1H), 3.70 (t, J = 2.3 Hz, 1H), 3.64 (m, 44H), 3.37 (s, 3H), 2.58 (m, 2H), 2.50 (m, 2H), 1.98 (t, J = 2.6 Hz, 1H).

2.2.4. βCD-PEG_{5000}

βCD-$(N_3)_7$ (0.037 g, 0.028 mmol) and alkynyl-PEG_{5000} (1.1 g, 0.21 mmol) were dissolved in DMSO/water (7:1). $CuSO_4{\cdot}5H_2O$ (0.0053 g, 0.022 mmol) and ascorbic acid (0.0013 g, 0.066 mmol) were incorporated into the reaction. The mixture was stirred at 70 °C for 24 h and then concentrated under vacuum. The solid was re-dissolved in CH_2Cl_2 and 3-fold extracted with water to remove copper salts. The organic phase was collected and dried over Na_2SO_4. Finally, the product was purified by re-dissolving/re-precipitating with hexane/diethyl ether. After freeze-drying, βCD-PEG_{5000} was obtained as a white solid (0.9 g, 88%). $M_{n\text{-theo}}$: 36946.51; MALDI-TOF: m/z 37069.52.

2.2.5. βCD-PEG_{2000}

This reaction was carried out in a 3:1 DMSO/water mixture but was otherwise the same as in Section 2.2.4 with βCD-$(N_3)_7$ (0.04 g, 0.031 mmol), alkynyl-PEG_{2000} (0.49 g, 0.235 mmol), $CuSO_4{\cdot}5H_2O$ (0.006 g, 0.0235 mmol), and ascorbic acid (0.0014 g, 0.0705 mmol). The product was precipitated in excess of cold diethyl ether and freeze-dried. βCD-PEG_{2000} was obtained as a white solid (0.5 g, 99%). $M_{n\text{-theo}}$: 15973.95; MALDI-TOF: m/z 15413.38.

2.2.6. βCD-PEG_{550}

This reaction was carried out in a 2:1 DMSO/water mixture but was otherwise the same as in Section 2.2.4 with βCD-$(N_3)_7$ (0.033 g, 0.0251 mmol), alkynyl-PEG_{550} (0.124 g, 0.19 mmol); $CuSO_4{\cdot}5H_2O$ (0.005 g, 0.0193 mmol), and ascorbic acid (0.0012 g, 0.058 mmol). DMSO was removed and the crude product was re-dissolved in fresh CH_2Cl_2 to be then extracted with a saturated sodium chloride aqueous solution. The organic phase was dried over Na_2SO_4 and rota-evaporated

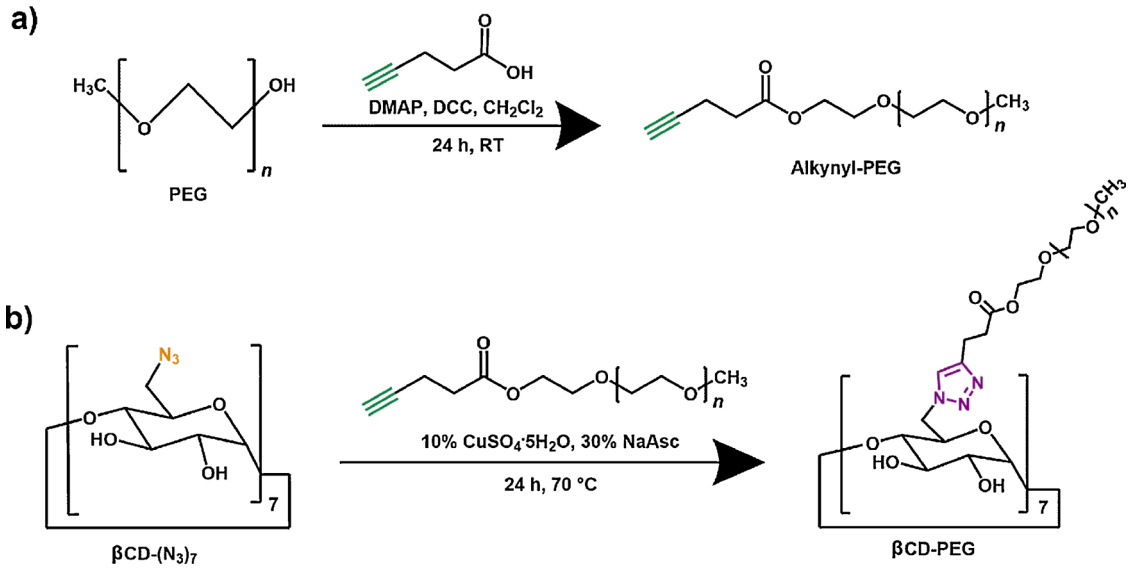

Scheme 1. General synthetic procedure for βCD-PEG systems.

to remove CH_2Cl_2. After freeze-drying, βCD-PEG_{550} was obtained as a brown semi-solid (0.08 g, 55%). $M_{n\text{-}theo}$: 5796.09; MALDI-TOF: *m/z* 5333.279.

2.3. Spectroscopy

Nuclear magnetic resonance (NMR) spectra were acquired at 25 °C on a Bruker Avance spectrometer (400 MHz) under Fourier transform mode. Fourier-transform infrared (FTIR) spectra were recorded on a Thermo Scientific Nicolet 6700 (4000–400 cm^{-1}). MALDI-TOF analyses were performed on a MicroFlex MALDI-TOF mass spectrometer (Bruker) equipped with a nitrogen UV laser (λ = 337 nm) pulsed at 20 Hz using linear acquisition mode and an accelerating potential of 20 kV. Mass spectra were acquired by accumulation of 720 laser shots for βCD-PEG_{5000}, βCD-PEG_{2000}, and βCD-PEG_{550}, respectively, and processed by Bruker Daltonics FlexAnalysis Software. The matrix consisted of a saturated solution of 2,5-dihydrobenzoic acid in water/acetonitrile/trifluoroacetic acid (40:60:0.1), and the final sample concentration was 0.3 mg/mL.

2.4. Biological assays

2.4.1. Cell cultures

HeLa and Vero cells were provided by Dr. Rosa Maria del Angel (Center for Research and Advanced Studies of the National Polytechnic Institute). Gibco DMEM Advanced growth medium was purchased from Fisher Scientific, and an MTS cell proliferation assay kit was acquired from Promega™.

Cell cultures of HeLa and Vero cells were grown in DMEM-advanced medium supplemented with 8% fetal bovine serum (FBS, Gibco™), 2× L-glutamine (Gibco™), and 1× penicillin-streptomycin (Gibco™). For in vitro viability experiments, cells were distributed in 96 well plates at 50,000 cells/well in DMEM-advanced medium supplemented with 8% FBS and 2× glutamine.

2.4.2. Isolation and culture of human peripheral blood monocytes

Human peripheral blood monocytes were isolated from buffy coats (collected from the blood bank at 20 de Noviembre-National Medical Center-ISSSTE, prior protocol authorization from Ethics Committee) from healthy donors using Histopaque-1077 (Sigma-Aldrich) following the manufacturer's instructions. Briefly, buffy coats and room-temperature-tempered Histopaque-1077 in a 2:1 ratio were placed in a 50 mL conical tube and centrifuged at 400 rpm for 30 min. The interface was collected and transferred to a fresh 50 mL conical tube with RPMI medium (Gibco™) supplemented with 10% FBS and 2× L-glutamine. Cells were distributed in plastic plates and incubated for 2 h at 37 °C in a humidified atmosphere with 5% CO_2 to allow monocyte adhesion. The medium was replaced every 48 h for 4 days, and non-adherent cells were removed in every exchange. For in vitro viability assays, cells were placed in a 96 well-plate at 50,000 cells per well in RPMI medium supplemented with 10% FBS and 2× L-glutamine. Peripheral blood monocytes were isolated from a different donor sample for each independent experiment.

2.4.3. In vitro cell viability assays

Experiments with HeLa, Vero, and human monocytes were carried out according to our previously reported protocol (López-Méndez et al., 2018). The three PEGylated structures, βCD, and free PEGs were evaluated at 25, 50, 100, 250, and 500 μg/mL.

2.4.4. Statistical analysis

Experimental data for HeLa and Vero cells were obtained from three independent experiments with three replicates each ($n = 9$). Two independent assays with three replicates each ($n = 6$) using human monocytes (from two different donors) were performed. In all cases, results are presented as mean ± S.D. Statistical comparison by analysis of variance was performed at a significance level of $p < 0.01$ and $p < 0.001$ based on a Student's *t*-test using GraphPad Prism.

3. Results and discussion

Alkynyl-PEGs were obtained through a Steglich esterification in high yields (Scheme 1a). The ^1H NMR of the modified PEGs revealed characteristic signals of the achieved products (Figs. S3–S5): a triplet corresponding to the terminal alkyne group proton (CH≡ C–) at 1.97, 1.90, and 1.98 ppm for alkynyl-PEG_{5000}, alkynyl-PEG_{2000}, and alkynyl-PEG_{550}, respectively; and two multiplets corresponding to (CH≡ CCH_2CH_2 C= O) at 2.5 and 2.57 ppm for the three alkynyl-PEGs. NMR was also used to calculate the functionalized PEG molecular weights (Izunobi & Higginbotham, 2011). The NMR number-average molecular weight ($M_{n\text{-}NMR}$) of the three alkynyl-PEGs was calculated from the peak area ratio of the PEG repeating unit (CH_2CH_2O) at 3.6 ppm and terminal group ($CH{\equiv}CCH_2CH_2C{=}O$) at ~2.5 ppm (Tables S1–S6). In all cases, $M_{n\text{-}NMR}$ was consistent with $M_{n\text{-}theo}$.

CuAAC reaction between alkynyl-PEGs and βCD-$(N_3)_7$ successfully yielded βCD-PEG_{5000}, βCD-PEG_{2000}, and βCD-PEG_{550} (Scheme 1b).

Although click reactions are robust, it is fundamental to establish appropriate experimental protocols for favorable click syntheses. The appropriate solvents, reaction time, and temperature will determine the success of the synthesis, especially when seven click reactions must occur simultaneously. Temperature was a crucial factor. Below 70 °C, reactions were incomplete, different degrees of substitutions and low yields were observed. On the other hand, at temperatures of both ~50 °C and ~90 °C, entities of several molecular weights, different to those corresponding to a certain degree of substitution, were observed for βCD-PEG_{5000} and βCD-PEG_{2000}. Those structures presumably correspond to inclusion complexes between PEG and βCD (data not shown). The total solvent volume was also necessary to control, as longer PEG chains required higher dilution. Once the appropriate reactions were established, the three products were quantitatively obtained.

MALDI-TOF analysis provided the molecular weights of the PEGylated structures and, therefore, the substitution degree and architecture of the modified macrocycle. The *m/z* values were compared with the expected theoretical M_n calculated as: $M_{n\text{-theo}}$ βCDPEG = 1015.91 (βCD core) + 469.42 (triazole) + 7 x PEG ($[PEG]_RCOOCH_2CH_2$; where R = polymer repeat units). By considering *m/z* values and relative peak intensities of MALDI-TOF spectra, the degree of substitution and subsequently the scope of our click chemistry protocol to PEGylate the seven primary-face reactive positions of βCD were analyzed.

According to Fig. 2a, βCD-PEG_{5000} was obtained as a mixture, where the most abundant peak corresponds to the heptasubstituted structure and the other represents a hexasubstituted product. Similarly, βCD-PEG_{2000} had two products with hepta and hexa substitution patterns. A small proportion of βCD bearing 4 PEG arms was also observed. For both βCD-PEG_{5000} and βCD-PEG_{2000}, the 7 PEG arm structure predominated (Fig. 2b). The coupling of PEG_{550} to the seven βCD primary face positions was successfully achieved, as only one peak representing heptasubstituted βCD-PEG_{550} was observed (Fig. 2c) although the yield was the lower out of the three systems. The fact that alkynyl-PEG chain lengths sterically hinder their own attachment to all the azide functionalities of βCD-$(N_3)_7$ could explain our findings.

A low-intensity peak, indicating the association of two structures (dimers), was observed in all three spectra. Native and polymeric βCDs are prone to aggregation and self-assembly processes, which is of importance because such processes could affect their complexing abilities and supramolecular behavior on one hand. On the other, they can induce the formation of micellar-type aggregates, which will lead to improved solubilizing properties (Collins et al., 2013; Messner, Kurkov, Jansook, & Loftsson, 2010; Zhang & Ma, 2013). Therefore, detailed investigation on the aggregation behavior of the PEGylated CDs would be very significant.

3.1. Biological experiments

The design and development of materials for drug delivery applications is an appealing pursuit, as they are expected to maximize the efficacy of drugs and improve diagnoses. Despite extensive research, its translation to clinical practice remains limited. This is partially due to the narrow understanding of the relationship between the material physicochemical properties and specific biological responses. Hydrophobicity, hydrophilicity, aggregation, size, shape, and surface properties have been shown to determine material cell internalization and biological responses originating from material-cell interactions (Pelaz et al., 2017). Like our PEGylated CDs, many materials are designed to carry bioactive molecules, and it is vital to systematically investigate their interaction with bio-interfaces at an early development stage. βCD and PEG are typically considered safe components. Nevertheless, βCDPEG systems are new chemical entities with different physicochemical features and it should not be assumed that βCDPEG systems have the same biological behavior than their parent compounds.

3.1.1. Vero cells

Fig. 3a shows that the PEGylated materials did not alter the viability of Vero cells at any evaluated concentration. βCD and free PEGs did not affected Vero cells viability either (Table S7).This agrees with previous reports, where neither βCD derivatives nor PEG-coated materials affected these cells viability (Díaz-Moscoso et al., 2010; Rusen et al., 2016; Silva et al., 2016).

3.1.2. HeLa cells

The effect of PEG, βCD, and βCDPEGs on HeLa cells viability was evaluated (Fig. 3b). HeLa cells were not affected by βCD (Table S8). This result agrees with a recent report showing that βCD exerts cytotoxicity in HeLa cells only at concentrations above 3 mM (Szente, Singhal, Domokos, & Song, 2018). Free PEGs did not alter HeLa cells either. Similar results were observed for βCD-PEG_{2000} and βCD-PEG_{5000} (Table S8). Surprisingly, we found that βCD-PEG_{550} had a significant effect on HeLa cells viability (Tables 1 and S9). As free PEG_{550} was innocuous, this may arise from the final architecture of the polymeric structure, along with PEG density caused by the spatial closeness of the polymer chains attached to the βCD primary face.

Previously, an evaluation of a series of linear PEG derivatives, including PEG methyl ether acrylate (mPEGA) and PEG methyl ether methacrylate (mPEGMA) on HeLa cells revealed a toxic effect that varied in severity depending on chain terminal group and polymer molecular weight (Liu et al., 2017). Notably, Liu et al. reported that mPEGMA (M_w 500) and mPEGA480 (M_w 480) exerted the highest toxicities, with the latter showing a 20% viability at a concentration of 0.4 mg/mL. Here, 24% of HeLa cells remained viable when exposed to βCD-PEG_{550} at 0.5 mg/mL. Although βCD-PEG_{550} structurally differs from PEGMA and PEGA, the similar results between the two studies are interesting considering that they concern polymers of comparable molecular weights.

3.1.3. Human monocytes

The effect of the three PEGylated βCDs on primary cells, namely human monocytes, was investigated (Fig. 3c). We found that neither βCD nor PEGs affected monocytes viability. Similar results were observed for βCD-PEG_{2000} and βCD-PEG_{5000} (Table S10). However, βCD-PEG_{550} at 500 μg/mL impaired monocytes viability by 60% (Tables 1 and S11). This result is in accordance with the βCD-PEG_{550} effect on HeLa cells (Fig. S2). As discussed, the difference between free PEG_{550} and βCD-PEG_{550} may arise from the distinct architecture of PEG_{550} and a change in polymer density upon partial coating of βCD.

βCD and PEG are typically considered safe components. Nevertheless, PEGylated βCDs comprise new entities displaying different chemical features, sizes, and architectures, aspects to which cells are sensitive (Foroozandeh & Aziz, 2018). PEG is particularly interesting as hypersensitivity, toxicity, and an antagonism in its stealth effect depend on polymer density, architecture, molecular weight, and functional moieties (Kelley et al., 2018; Knop et al., 2010; Liu et al., 2017).

These intriguing results inspire for, in first place, investigating the cells death mechanisms. Subsequently, an extensive study on the βCD-PEG_{550} effect regarding adhesion, differentiation, and cytokine activation in human monocytes will provide relevant information for the potential of βCDPEG structures in the drug delivery field and for the relationship PEG structure-cellular response regarding PEGylation approach. βCD-PEG_{5000}, and βCD-PEG_{2000} should not be excluded for further research as they could be altering cellular responses at molecular level, without necessarily causing cell death. The same as βCD and PEG, as they have been reported to alter in some extent monocytes adhesion and their response to inflammatory stimuli (Ao, Wu, Zhou, & Chen, 2016; Bakke et al., 2017; Matassoli et al., 2018; Wagner & Bryers, 2003).

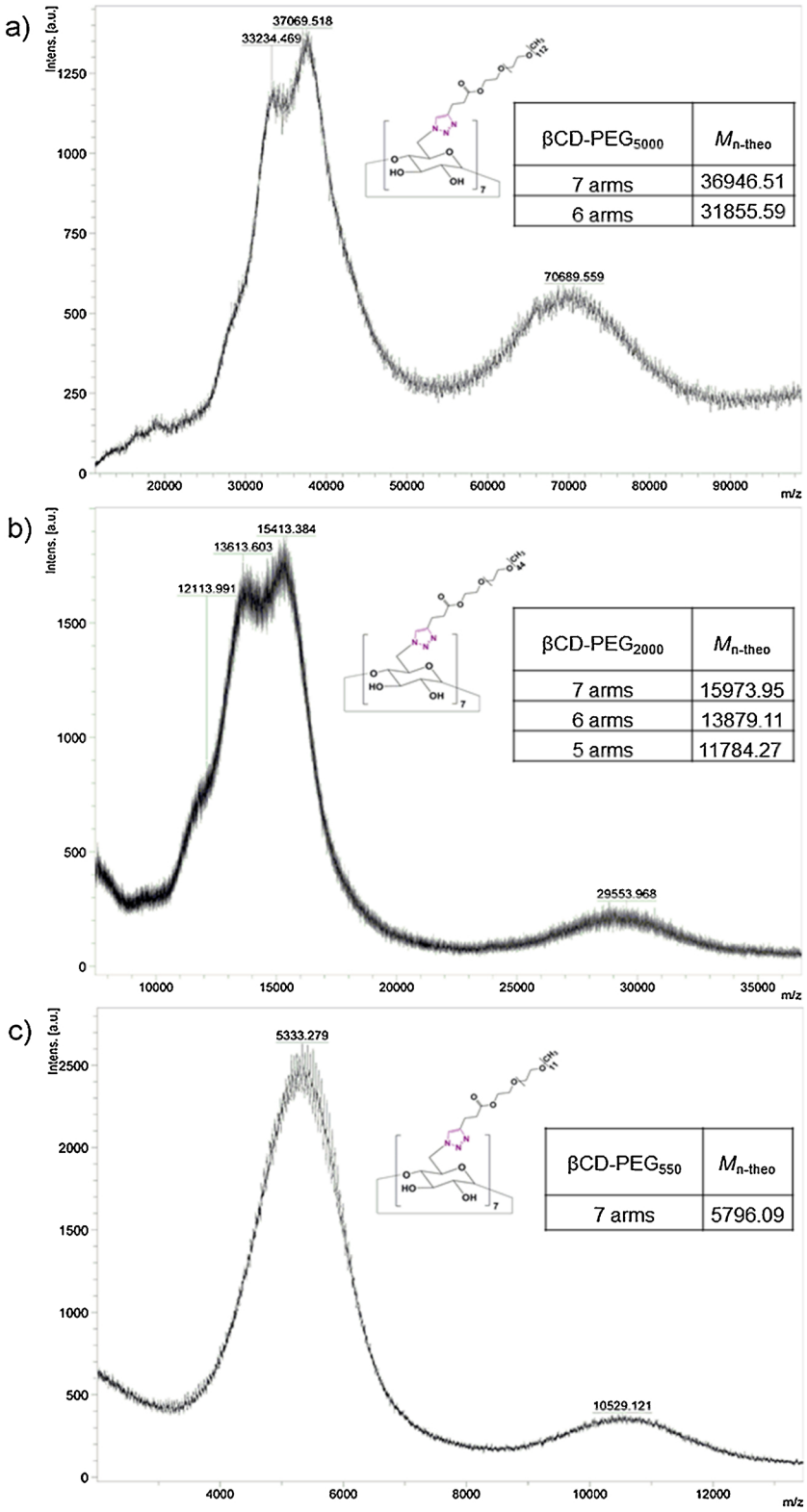

Fig. 2. MALDI-TOF spectra of βCD-PEG$_{550}$, βCD-PEG$_{2000}$, and βCD-PEG$_{5000}$.

4. Conclusions

PEGs of different molecular weight were conjugated to the βCD primary face by click reactions. Both βCD-PEG$_{2000}$ and βCD-PEG$_{5000}$ were achieved in high yields with the heptasubstituted product predominating over the product with six PEG chains. On the other hand, the CuAAC reaction yielded heptasubstituted βCD-PEG$_{550}$ as the only detectable product. Thus, click chemistry was a suitable tool to obtain the three star-shaped PEGylated βCD structures in quantitative yields, which confirms the previously stated hypothesis. As the PEGylated CDs are intended for further application as drug carriers, it was mandatory to investigate their interaction with bio-interfaces before drug loading.

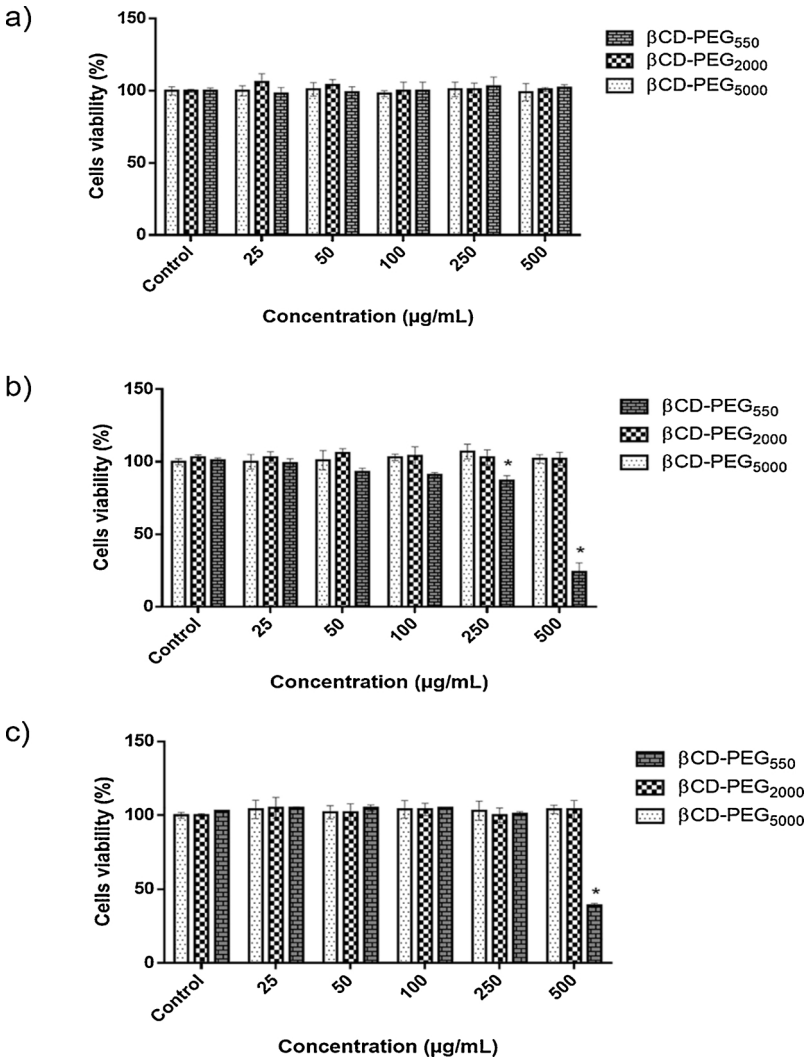

Fig. 3. Effect of βCD-PEG systems on a) Vero and b) HeLa cell viability (*=$p < 0.01$) and c) human monocytes (*=$p < 0.001$).

Table 1
Effect of βCD-PEG_{550} on HeLa cells and human monocytes viability.

Concentration µg/mL	Cell viability (%) ± SD	
	HeLa	Human monocytes
25	99 ± 3.0	105 ± 0.7
50	93 ± 2.5	105 ± 2.1
100	91 ± 1.5	105 ± 0.0
250	87 ± 3.5	101 ± 1.4
500	24 ± 6.2	39 ± 1.4
Control	101 ± 1.7	103 ± 0.0

βCDPEG structures did not affect Vero cells. However, of the three systems, βCD-PEG_{550} reduced HeLa cells and human monocytes viability, being the former more sensitive than the latter. In this case, the resulting material displayed a different biological interaction than its precursors, confirming our second hypothesis. The overall results are a motivation to investigate cell death mechanisms in HeLa and human monocytes models. Additionally, adhesion, differentiation, and cytokine secretion studies will provide valuable information about the interactions of PEGylated materials with phagocytic cells.

Despite the popularity of the PEGylation approach, our results underscore the importance of careful and systematic design of PEGylated materials for future use in drug delivery systems.

Declaration of Competing Interest

None.

Acknowledgements

Y. Rojas-Aguirre acknowledges the financial support to Materials Research Institute, UNAM (Project 1306) and PAPIIT-UNAM (IA200919); to Lorena Jáuregui-Solares for the elaboration of the graphical abstract; and specially thanks to Prof. Y. Yüksel-Durmaz for her mentorship, guidance and click chemistry and polymers topics exciting discussions. L. J. López-Méndez thanks to CONACyT for the Ph.D scholarship (336116) and P. Guadarrama thanks to CONACyT Project 239672. All authors thank to M. Sc. Carlos Ramos Vilchis for their assistance in setting up the vacuum systems required for the synthetic work; M. Sc. Lucero Rios Ruiz and Q. Eréndira García Ríos for MALDI-MS experiments; and M. Sc. Gerardo Cedillo Valverde for NMR spectra acquisition.

Appendix A. Supplementary data

Supplementary material related to this article can be found, in the online version, at doi:https://doi.org/10.1016/j.carbpol.2019.115113.

References

Anselmo, A. C., & Mitragotri, S. (2016). Nanoparticles in the clinic. *Bioengineering & Translational Medicine, 1*(1), 10–29. https://doi.org/10.1002/btm2.10003.

Antoniuk, I., & Amiel, C. (2016). Cyclodextrin-mediated hierarchical self-assembly and its potential in drug delivery applications. *Journal of Pharmaceutical Sciences, 105*(9), 2570–2588. https://doi.org/10.1016/j.xphs.2016.05.010 September 1 Elsevier.

Ao, M., Wu, L., Zhou, X., & Chen, Y. (2016). Methyl-β-Cyclodextrin impairs the monocyte-adhering ability of endothelial cells by down-regulating adhesion molecules and Caveolae and reorganizing the actin cytoskeleton. *Biological & Pharmaceutical Bulletin, 39*(6), 1029–1034. https://doi.org/10.1248/bpb.b16-00047.

Bakke, S. S., Aune, M. H., Niyonzima, N., Pilely, K., Ryan, L., Skjelland, M., ... Espevik, T. (2017). Cyclodextrin reduces cholesterol crystal–induced inflammation by modulating complement activation. *The Journal of Immunology, 199*(8), 2910–2920. https://doi.org/10.4049/jimmunol.1700302.

Barenholz, Y. (2012). Doxil®—The first FDA-approved nano-drug: Lessons learned. *Journal of Controlled Release, 106*(2), 117–134. https://doi.org/10.1016/j.jconrel.2012.03.020 June 10 Elsevier.

Buckwalter, D. J., Sizovs, A., Ingle, N. P., & Reineke, T. M. (2012). MAG versus PEG: Incorporating a poly(MAG) layer to promote colloidal stability of nucleic acid/"click cluster" complexes. *ACS Macro Letters, 1*(5), 609–613. https://doi.org/10.1021/mz300081d.

Collins, C. J., McCauliff, L. A., Hyun, S. H., Zhang, Z., Paul, L. N., Kulkarni, A., ... Thompson, D. H. (2013). Synthesis, characterization, and evaluation of pluronic-based β-cyclodextrin polyrotaxanes for mobilization of accumulated cholesterol from Niemann-Pick type C fibroblasts. *Biochemistry, 52*(19), 3242–3253. https://doi.org/10.1021/bi3010889.

Davis, M. E. (2009). The first targeted delivery of siRNA in humans via a self-assembling, cyclodextrin polymer-based nanoparticle: From concept to clinic. *Molecular Pharmaceutics, 6*(3), 659–668. https://doi.org/10.1021/mp900015y.

Díaz-Moscoso, A., Vercauteren, D., Rejman, J., Benito, J. M., Ortiz Mellet, C., De Smedt, S. C., ... Fernández, J. M. G. (2010). Insights in cellular uptake mechanisms of pDNA-polycationic amphiphilic cyclodextrin nanoparticles (CDplexes). *Journal of Controlled Release, 143*(3), 318–325. https://doi.org/10.1016/j.jconrel.2010.01.016.

do Nascimento, M. H. M., Ferreira, M., Malmonge, S. M., & Lombello, C. B. (2017). Evaluation of cell interaction with polymeric biomaterials based on hyaluronic acid and chitosan. *Journal of Materials Science: Materials in Medicine, 28*(5), https://doi.org/10.1007/s10856-017-5875-x.

Dos Santos, N., Allen, C., Doppen, A. M., Anantha, M., Cox, K. A. K., Gallagher, R. C., ... Bally, M. B. (2007). Influence of poly(ethylene glycol) grafting density and polymer length on liposomes: Relating plasma circulation lifetimes to protein binding. *Biochimica et Biophysica Acta - Biomembranes, 1768*(6), 1367–1377. https://doi.org/10.1016/j.bbamem.2006.12.013.

Farace, C., Sánchez-Moreno, P., Orecchioni, M., Manetti, R., Sgarrella, F., Asara, Y., ... Delogu, L. G. (2016). Immune cell impact of three differently coated lipid nanocapsules: Pluronic, chitosan and polyethylene glycol. *Scientific Reports, 6*, 1–14. https://doi.org/10.1038/srep18423 (July 2015).

Faugeras, P.-A., Boëns, B., Elchinger, P.-H., Brouillette, F., Montplaisir, D., Zerrouki, R., & Lucas, R. (2012). When cyclodextrins meet click chemistry. *European Journal of Organic Chemistry, 2012*(22), 4087–4105. https://doi.org/10.1002/ejoc.201200013.

Foroozandeh, P., & Aziz, A. A. (2018). Insight into cellular uptake and intracellular trafficking of nanoparticles. *Nanoscale Research Letters, 13*(1), 339. https://doi.org/10.1186/s11671-018-2728-6.

Gadelle, A., & Defaye, J. (1991). Selective halogenation at primary positions of Cyclomaltooligosaccharides and a synthesis of Per-3,6-anhydro cyclomaltooligosaccharides. *Angewandte Chemie International Edition in English, 30*(1), 78–80. https://doi.org/10.1002/anie.199100781.

Gallego-Yerga, L., Benito, J. M., Blanco-Fernández, L., Martínez-Negro, M., Vélaz, I., Aicart, E., ... García Fernández, J. M. (2018). Plasmid-templated control of DNA–cyclodextrin nanoparticle morphology through molecular vector design for effective gene delivery. *Chemistry – A European Journal, 24*(15), 3825–3835. https://doi.org/10.1002/chem.201705723.

García Fernández, J., Ortiz Mellet, C., Jiménez Blanco, J., Fuentes Mota, J., Gadelle, A., Coste-Sarguet, A., & Defaye, J. (1995). Isothiocyanates and cyclic thiocarbamates of α, α′-trehalose, sucrose, and cyclomaltooligosaccharides. *Carbohydrate Research, 268*(1), 57–71. https://doi.org/10.1016/0008-6215(94)00312-4.

Godinho, B. M. D. C., Ogier, J. R., Quinlan, A., Darcy, R., Griffin, B. T., Cryan, J. F., & Caitriona, M. O. D. (2014). PEGylated cyclodextrins as novel siRNA nanosystems: Correlations between polyethylene glycol length and nanoparticle stability. *International Journal of Pharmaceutics, 473*(1–2), 105–112. https://doi.org/10.1016/j.ijpharm.2014.06.054.

Grenier, P., Viana, I. M., de, O., Lima, E. M., & Bertrand, N. (2018). Anti-polyethylene glycol antibodies alter the protein corona deposited on nanoparticles and the physiological pathways regulating their fate in vivo. *Journal of Controlled Release, 287*(August), 121–131. https://doi.org/10.1016/j.jconrel.2018.08.022.

He, X. P., Zeng, Y. L., Zang, Y., Li, J., Field, R. A., & Chen, G. R. (2016). Carbohydrate CuAAC click chemistry for therapy and diagnosis. *Carbohydrate Research, 429*, 1–22. https://doi.org/10.1016/j.carres.2016.03.022 June 24 Elsevier.

Hu, Q., Tang, G., & Chu, P. K. (2014). Cyclodextrin-based host − guest supramolecular nanoparticles for delivery: From design to applications. *Accounts of Chemical Research, 47*, 2017–2025. https://doi.org/10.1021/ar500055s.

Izunobi, J. U., & Higginbotham, C. L. (2011). Polymer molecular weight analysis by 1H NMR spectroscopy. *Journal of Chemical Education, 88*(8), 1098–1104. https://doi.org/10.1021/ed100461v.

Jambhekar, S. S., & Breen, P. (2016). Cyclodextrins in pharmaceutical formulations I: Structure and physicochemical properties, formation of complexes, and types of complex. *Drug Discovery Today, 21*(2), 356–362. https://doi.org/10.1016/J.DRUDIS.2015.11.017.

Jiménez Blanco, J. L., Benito, J. M., Ortiz Mellet, C., & García Fernández, J. M. (2017). Molecular nanoparticle-based gene delivery systems. *Journal of Drug Delivery Science and Technology, 42*, 18–37. https://doi.org/10.1016/j.jddst.2017.03.012.

Kelley, W. J., Fromen, C. A., Lopez-Cazares, G., & Eniola-Adefeso, O. (2018). PEGylation of model drug carriers enhances phagocytosis by primary human neutrophils. *Acta Biomaterialia, 79*, 283–293. https://doi.org/10.1016/j.actbio.2018.09.001.

Khan, A. R., Forgo, P., Stine, K. J., & D'Souza, V. T. (1998). Methods for selective modifications of cyclodextrins. *Chemical Reviews, 98*(5), 1977–1996. https://doi.org/10.1021/cr970012b.

Knop, K., Hoogenboom, R., Fischer, D., & Schubert, U. S. (2010). Poly(ethylene glycol) in drug delivery: Pros and cons as well as potential alternatives. *Angewandte Chemie - International Edition, 49*(36), 6288–6308. https://doi.org/10.1002/anie.200902672.

Li, R.-Y., Liu, Z.-G., Liu, H.-Q., Chen, L., Liu, J.-F., & Pan, Y.-H. (2015). Evaluation of biocompatibility and toxicity of biodegradable poly (DL-lactic acid) films. *American Journal of Translational Research, 7*(8), 1357–1370. Retrieved from http://www.ncbi.nlm.nih.gov/pubmed/26396667%0Ahttp://www.pubmedcentral.nih.gov/articlerender.fcgi?artid=PMC4568792.

Liu, G., Li, Y., Yang, L., Wei, Y., Wang, X., Wang, Z., & Tao, L. (2017). Cytotoxicity study of polyethylene glycol derivatives. *RSC Advances, 7*(30), 18252–18259. https://doi.org/10.1039/c7ra00861a.

López-Méndez, L. J., González-Méndez, I., Aguayo-Ortiz, R., Dominguez, L., Alcaraz-Estrada, S. L., Rojas-Aguirre, Y., & Guadarrama, P. (2018). Synthesis of a poly(ester) dendritic β-cyclodextrin derivative by "click" chemistry: Combining the best of two worlds for complexation enhancement. *Carbohydrate Polymers, 184*(1), 20–29. https://doi.org/10.1016/J.CARBPOL.2017.12.049.

Matassoli, F. L., Leão, I. C., Bezerra, B. B., Pollard, R. B., Lütjohann, D., Hildreth, J. E. K., & de Arruda, L. B. (2018). Hydroxypropyl-beta-cyclodextrin reduces inflammatory signaling from monocytes: Possible implications for suppression of HIV chronic immune activation. *mSphere, 3*(6), 1–13. https://doi.org/10.1128/msphere.00497-18.

Meghani, N. M., Amin, H. H., & Lee, B. J. (2017). Mechanistic applications of click chemistry for pharmaceutical drug discovery and drug delivery. *Drug Discovery Today, 22*(11), 1604–1619. https://doi.org/10.1016/j.drudis.2017.07.007.

Mellet, C. O., Fernández, J. M. G., & Benito, J. M. (2011). Cyclodextrin-based gene delivery systems. *Chemical Society Reviews, 40*(3), 1586–1608. https://doi.org/10.1039/C0CS00019A.

Messner, M., Kurkov, S. V., Jansook, P., & Loftsson, T. (2010). Self-assembled cyclodextrin aggregates and nanoparticles. *International Journal of Pharmaceutics, 387*(1–2), 199–208. https://doi.org/10.1016/j.ijpharm.2009.11.035.

O'Mahony, A. M., Ogier, J., Desgranges, S., Cryan, J. F., Darcy, R., & O'Driscoll, C. M. (2012). A click chemistry route to 2-functionalised PEGylated and cationic β-cyclodextrins: Co-formulation opportunities for siRNA delivery. *Organic & Biomolecular Chemistry, 10*(25), 4954–4960. https://doi.org/10.1039/c2ob25490e.

Owens, D. E., & Peppas, N. A. (2006). Opsonization, biodistribution, and pharmacokinetics of polymeric nanoparticles. *International Journal of Pharmaceutics, 307*(1), 93–102. https://doi.org/10.1016/j.ijpharm.2005.10.010.

Pelaz, B., Alexiou, C., Alvarez-Puebla, R. A., Alves, F., Andrews, A. M., Ashraf, S., ... Parak, W. J. (2017). Diverse applications of nanomedicine. *ACS Nano, 11*(3), 2313–2381. https://doi.org/10.1021/acsnano.6b06040.

Pelegrino, M. T., de A. Lima, B., do Nascimento, M. H. M., Lombello, C. B., Brocchi, M., & Seabra, A. B. (2018). Biocompatible and antibacterial nitric oxide-releasing pluronic F-127/Chitosan hydrogel for topical applications. *Polymers, 10*(4), https://doi.org/10.3390/polym10040452.

Renero-Lecuna, C., Iturrioz-Rodríguez, N., González-Lavado, E., Padín-González, E., Navarro-Palomares, E., Valdivia-Fernández, L., ... González-Legarreta, L. (2019). Effect of size, shape, and composition on the interaction of different nanomaterials with HeLa cells. *Journal of Nanomaterials, 2019*, 1–11. https://doi.org/10.1155/2019/7518482.

Řezanka, M. (2018). Synthesis of substituted cyclodextrins. *Environmental Chemistry Letters, 17*(1), 49–63. https://doi.org/10.1007/s10311-018-0779-7.

Richards, D. M., & Endres, R. G. (2014). The mechanism of phagocytosis: Two stages of engulfment. *Biophysical Journal, 107*(7), 1542–1553. https://doi.org/10.1016/j.bpj.2014.07.070.

Rusen, L., Neacsu, P., Cimpean, A., Valentin, I., Brajnicov, S., Dumitrescu, L. N., ... Dinescu, M. (2016). In vitro evaluation of poly(ethylene glycol)-block-poly(ε-caprolactone) methyl ether copolymer coating effects on cells adhesion and proliferation. *Applied Surface Science, 374*, 23–30. https://doi.org/10.1016/j.apsusc.2015.08.214.

Schmidt, B. V. K. J., Hetzer, M., Ritter, H., & Barner-Kowollik, C. (2014). Complex macromolecular architecture design via cyclodextrin host/guest complexes. *Progress in Polymer Science, 39*(1), 235–249. https://doi.org/10.1016/j.progpolymsci.2013.09.006.

Silva, C. V. N. S., Barbosa, J. A. P., Ferraz, M. S., Silva, N. H., Honda, N. K., Rabello, M. M., ... Santos-Magalhães, N. S. (2016). Molecular modeling and cytotoxicity of diffractaic acid: HP-β-CD inclusion complex encapsulated in microspheres. *International Journal of Biological Macromolecules, 92*, 494–503. https://doi.org/10.1016/j.ijbiomac.2016.06.073.

Simões, S. M. N., Rey-Rico, A., Concheiro, A., & Alvarez-Lorenzo, C. (2015). Supramolecular cyclodextrin-based drug nanocarriers. *Chemical Communications, 51*(29), 6275–6289. https://doi.org/10.1039/c4cc10388b.

Sun, T., Zhang, Y. S., Pang, B., Hyun, D. C., Yang, M., & Xia, Y. (2014). Engineered nanoparticles for drug delivery in cancer therapy. *Angewandte Chemie - International Edition, 53*(46), 12320–12364. https://doi.org/10.1002/anie.201403036.

Szente, L., Singhal, A., Domokos, A., & Song, B. (2018). Cyclodextrins: Assessing the impact of cavity size, occupancy, and substitutions on cytotoxicity and cholesterol

homeostasis. *Molecules, 23*(5), 1–15. https://doi.org/10.3390/molecules23051228.
Wagner, V. E., & Bryers, J. D. (2003). Monocyte/macrophage interactions with base and linearand star-like PEG-modified PEG-poly(acrylic acid) co-polymers. *Journal of Biomedical Materials Research - Part A, 66*(1), 62–78. https://doi.org/10.1002/jbm.a.10516.
Yang, Q., Jones, S. W., Parker, C. L., Zamboni, W. C., Bear, J. E., & Lai, S. K. (2014). Evading immune cell uptake and clearance requires PEG grafting at densities substantially exceeding the minimum for brush conformation. *Molecular Pharmaceutics, 11*(4), 1250–1258. https://doi.org/10.1021/mp400703d.
Zhang, J., & Ma, P. X. (2013). Cyclodextrin-based supramolecular systems for drug delivery: Recent progress and future perspective. *Advanced Drug Delivery Reviews, 65*(9), 1215–1233. https://doi.org/10.1016/j.addr.2013.05.001.
Zhang, P., Sun, F., Liu, S., & Jiang, S. (2016). Anti-PEG antibodies in the clinic: Current issues and beyond PEGylation. *Journal of Controlled Release, 244*, 184–193. https://doi.org/10.1016/j.jconrel.2016.06.040.